Isolation of Contributions of Residual Stress and Weld Microstructure to Fatigue Crack Growth Rates in Welds

Rui Bao[1,*], Ning Tang[1], Xiang Zhang[2]

[1] Institute of Solid Mechanics, School of Aeronautic Science and Engineering, Beihang University, Beijing, 100191, P.R. China
[2] Department of Aerospace Engineering, School of Engineering, Cranfield University, Bedford, MK43 0AL, U.K.
* Corresponding author: rbao@buaa.edu.cn

Abstract   Weld residual stresses and microstructural changes show coupled effects on fatigue crack growth rates resulting in more difficulties and complexity in crack growth life analysis for weld joints. Uncoupling these effects is a desirable option for understanding the influence of each factor and establishing more accurate crack growth prediction methods. A method for isolating the contributions of residual stress and weld microstructure change to fatigue crack growth rates in welds is presented in this paper. The proposed method is based on the superposition rule in fracture mechanics. Example of fusion weld specimens of different configurations and subjected to different loading conditions are presented to demonstrate the procedure of the method. Factors that will influence the solution, such as the applied and residual stress intensity factors, effective stress intensity factor ratio, choice of crack growth laws etc. are assessed and discussed in details.

Keywords   Fatigue crack growth rate, Weld, Residual stress, Microstructural change, Isolation

1. Introduction

The application of advanced welding technologies to fabricate aircraft structural components is recognized as one of the most promising methods to achieve further structure weight reduction and manufacture cost saving, which requires a step change in the structural integrity assessment and, consequently, sets new challenges to the damage tolerance evaluation for welded joints. Crack growth life estimation is one of the key tasks in damage tolerance assessment. Welding procedure will introduce micro-structural changes as well as weld residual stress (RS), both of which have shown significant effects on fatigue crack growth (FCG) rates. Significant amount of research has been conducted in the past 20 years to understand the crack growth behaviors in aerospace aluminum alloys joined by different advanced welding technologies, e.g. fusion, laser and friction stir welding (FSW), which have different characteristics in RS levels and microscopic texture [1-9].

Effects of microstructure and residual stress on FCG depend on the relative positions of the crack to the weld zone. Tests on specimens with crack parallel to the weld line indicate that the growth rate in the regime with low hardness is much slower and of higher threshold [10, 11], while it is not always the same for longitudinal welded specimen (crack propagates perpendicular to the weld line). Fratini et al. [4] presented similar results in the study on longitudinal welded 2024-T351 aluminum alloy showing changes in microstructure and hardness play a major role in the fusion zone (FZ) and residual stresses take the first place outside the FZ. Pouget et al. [9] predicted crack growth rate in longitudinal FSW 2050 aluminum alloy by finite element simulation showing that the material parameters in FZ could have significant effects on predicting results. Therefore, it is a common practice that only the primary influential factor is considered in crack growth analysis of welds. For example, studies [7, 12-14] have concluded that RS plays a major role on the FCG rates for crack propagation perpendicular to a weld, consequently, superposition rule is adopted in this case to account for the combined effects of residual and applied stresses on crack growth, microstructural changes effect, although present obviously in weld nugget, is ignored. For crack propagation within

and parallel to a weld, crack growth rates have been found to be considerably lower than that in the base material (BM) [11]; effect of microstructural and hardness changes on FCG rate is most important and hence must be considered in this circumstance. However, in most cases, both microstructural change and residual stresses contribute to the change in crack growth rate in welds compared with that in the BM, and the two contributions couple each other [4,9,10,15]; neglecting any of the two (to simplify the crack growth analysis procedure) will result in inaccurate analysis.

On the other hand, it is well-known that RS magnitude and distribution are different for different dimensions, but the weld metal (WM) microstructural change should be the same for the same welding process parameters even though the dimensions of the test coupon and component are different. If the coupled effects on FCG rate can be isolated, it will provide a more accurate analysis tool for predicting crack growth life, and have wider applicability.

A method for isolating the contributions of RS and weld micro-structure change to fatigue crack growth in welds is presented in this paper, which is based on the superposition rule in fracture mechanics. An example of VPPA (Variable Polarity Plasma Arc) welded specimens is presented to demonstrate the isolation procedure. The characteristic parameter, i.e. stress intensity factors due to residual and applied stresses, is calculated by finite element method. Factors which will influence the results, such as applied and residual stress intensity factors, effective stress intensity factor ratio, choice of crack growth laws, etc. are assessed and discussed in details.

2. Methodology for Isolating the Contributing Factors

2.1. Basic idea

The difference in the crack growth rate between the WM and the BM is:

$$\Delta = \left(da/dN\right)_w - \left(da/dN\right)_b \qquad \backslash* \text{ MERGEFORMAT (1)}$$

where $\left(da/dN\right)_w$ and $\left(da/dN\right)_b$ are the crack growth rates in the WM and BM respectively.

The difference Δ is the summation of the two contributing parts; one arises from weld residual stresses, labeled as Δ_1, and the other is due to the microstructural change introduced by the welding process, marked as Δ_2. Fig. 1 shows schematically the changes in crack growth rate consisting of Δ_1 and Δ_2. These increments, Δ, Δ_1 and Δ_2, can be either positive or negative and may not be kept the same with the increase of the stress intensity factor range ΔK.

As mentioned, Δ_1, arising from the residual stress, is associated with the configuration of the weld component, and Δ_2 depends only on the weld process parameters. If Δ_1 and Δ_2 can be obtained respectively, the contributions of residual stress and microstructural change on crack growth can be isolated.

2.2. Method for determining Δ_1

Since Δ_1 arises from RS, it is reasonable to assume that a weld procedure introduces residual stress only without changing the microstructure. The crack growth rate in this case is:

$$\left(da/dN\right)_R = \left(da/dN\right)_b + \Delta_1 \qquad (2)$$

where $(\mathrm{d}a/\mathrm{d}N)_b$ is the crack growth rate in the BM subjected to externally applied load, and can be correlated by stress intensity factor range ΔK, stress ratio R, and material property constants A_1, A_2, …, A_n. Commonly used correlation equations are the Paris, Walker, Forman, and NASGRO equations etc. [16]. A general form of these laws can be expressed by Eq. (3), where $(\mathrm{d}a/\mathrm{d}N)_R$ is the crack growth rate due to the combined applied stress and RS. Because there is no material property change, the superposition rule [17] can be used reasonably, and $(\mathrm{d}a/\mathrm{d}N)_R$ can be found by Eq. (4).
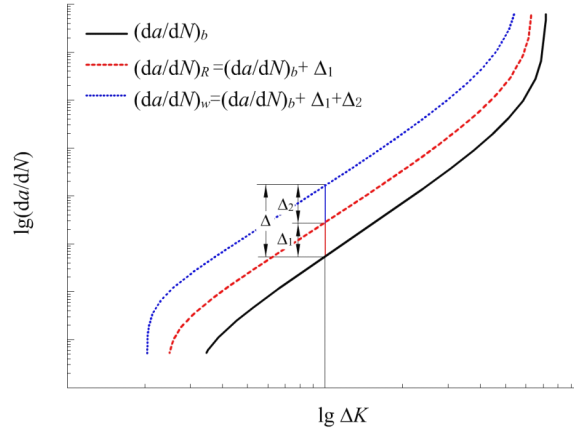
Fig. 1. Schematic of contribution of weld RS and material property change to FCG rate in WM

$$\left(da/dN \right)_b = f\left(\Delta K_{app}, R_{app}, A_1, \cdots, A_n \right) \tag{3}$$

$$\left(da/dN \right)_R = f\left(\Delta K_{tot}, R_{eff}, A_1, \cdots, A_n \right) \tag{4}$$

where ΔK_{app} and ΔK_{tot} are the stress intensity factor range due to the applied and total (applied + residual) stresses, respectively. R_{app} and R_{eff} are the stress intensity factor ratios due to the applied and total stress, respectively.

$$\Delta K_{tot} = K_{tot\,max} - K_{tot\,min} = \left(K_{app\,max} + K_{res} \right) - \left(K_{app\,min} + K_{res} \right) = \Delta K_{app} \tag{5}$$

$$R_{eff} = \frac{K_{app\,min} + K_{res}}{K_{app\,max} + K_{res}} \tag{6}$$

K_{res} is the stress intensity factor due to the RS, which can be calculated by either the finite element or weight function method [18]. Therefore, if the distribution of RS is available, both $(\mathrm{d}a/\mathrm{d}N)_b$ and $(\mathrm{d}a/\mathrm{d}N)_R$ can be calculated. Hence, Δ_1 could be obtained by:

$$\Delta_1 = \left(da/dN \right)_R - \left(da/dN \right)_b \tag{7}$$

2.3. Method for determining Δ_2

It may be imagined that if a weld procedure introduces no RS, then the only difference in crack growth rates between BM and WM is due to the change in material prosperities. In this case, the crack growth rate should be the intrinsic one which does not related to RS (in consequence to the specimen configuration):

$$\left(da/dN \right)_{Int} = \left(da/dN \right)_b + \Delta_2 \tag{8}$$

Since the change in crack growth rate is due to microstructural changes, $(\mathrm{d}a/\mathrm{d}N)_{int}$ cannot be estimated by the theory of macroscopic fracture mechanics. It cannot be measured either because no weld procedure will introduce zero RS. However, it is possible to estimate Δ_2 by Eq. (9) after Δ_1 is

determined.

$$\Delta_2 = \Delta - \Delta_1 = \left[\left(da/dN \right)_w - \left(da/dN \right)_b \right] - \left[\left(da/dN \right)_R - \left(da/dN \right)_b \right] = \left(da/dN \right)_w - \left(da/dN \right)_R \quad (9)$$

where $(da/dN)_w$ can be obtain by crack growth tests of WM specimens, quantity $(da/dN)_R$ could be determined by Eq. (4).

3. Demonstration Example of the Isolating Method

3.1. Introduction of the Example

Due to the availability of RS and FCG rate test data, 2024-T3 VPPA weld specimens are used as a demonstration example. The VPPA welding process was firstly investigated in 1940s and developed extensively in 1980s by the NASA for achieving high quality welds in aluminium alloys [19]. During the welding process, the molten pool and the heat input produce significant metallurgical changes compared with the BM. Both middle crack tension (MT) and compact tension (CT) specimens are used in this example. The specimen geometries are shown in Fig. 2. Measured RS distributions in the MT and CT specimens are given in Fig. 3 [7, 13]. For the configurations with longitudinal weld, crack grows across the fusion zone (FZ), heat affected zone (HAZ) and BM. The hardness in the FZ, where the molten material is solidified, is the lowest as this area contains a fairly coarse dendritic structure with little precipitation hardening [20]. Material in the HAZ has been thermally treated by the heat input during welding. These microstructure changes result in different crack growth rates comparing with that of the BM. FCG tests data are reported in [7, 21] and shown here in Fig. 4. Two applied loading conditions are considered, i.e. constant amplitude (CA) and constant ΔK (CK), of which $R = 0.1$ and 0.6 for the CA condition and $\Delta K = 6$, 11, and 15 MPa$\sqrt{m}$ for the CK condition.
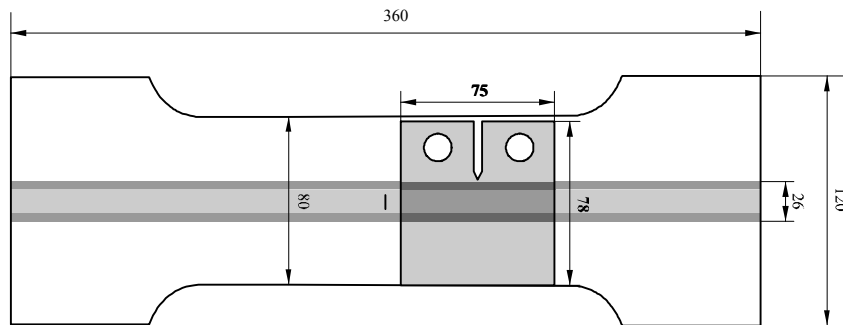
Fig. 2. MT and CT specimen configurations; CT is cut form an MT specimen [21]; unit: mm
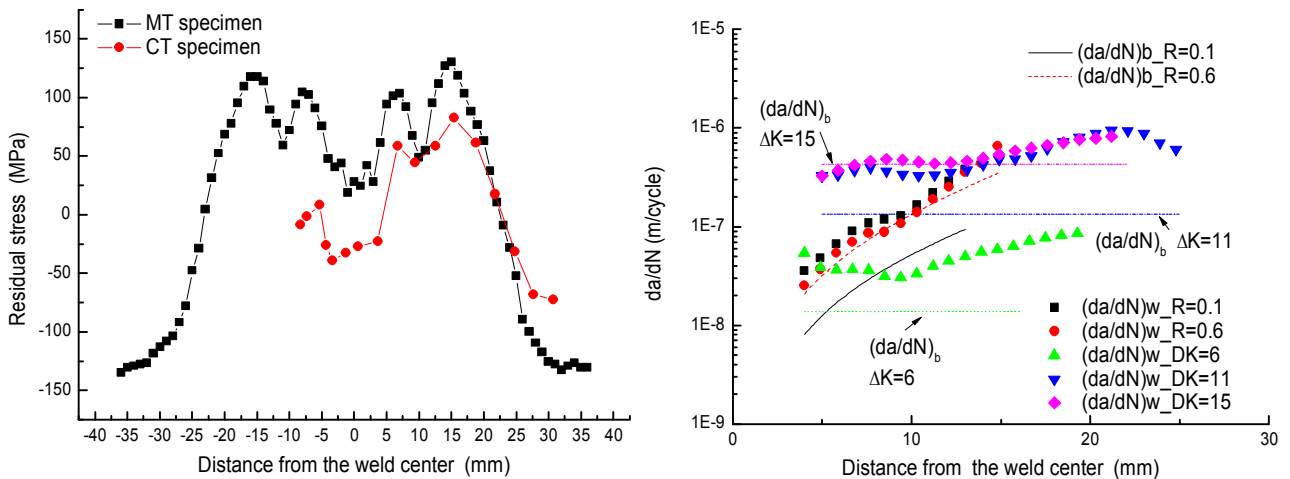
Fig 3.   Longitudinal RS distribution   Fig. 4. Measured crack growth rates in BM & WM

3.2. Estimation of Δ_1

Δ_1 can be evaluated by Eq. (7), in which, both $(da/dN)_b$ and $(da/dN)_R$ are calculated by the NASGRO equation [16] expressed in Eq. (10)-(12). For $(da/dN)_b$, ΔK and R corresponding to the externally applied load, whereas, for the calculation of $(da/dN)_R$, ΔK and R in the following equations should be replaced by ΔK_{tot} and R_{eff} as given in Eq. (5) and (6). While, the material constants used in the equations are kept unchanged of the BM according to the presented method, which are available in the data base of the software AFGROW.

$$\frac{da}{dN} = C\left[\left(\frac{1-f}{1-R}\right)\Delta K\right]^n \frac{\left(1-\frac{\Delta K_{th}}{\Delta K}\right)^p}{\left(1-\frac{K_{max}}{K_{crit}}\right)^q}, \tag{10}$$

$$f = \frac{K_{op}}{K_{max}} = \begin{cases} \max(R, A_0 + A_1 R + A_2 R^2 + A_3 R^3) & R \geq 0 \\ A_0 + A_1 R & -2 \leq R \leq 0 \\ a_0 - 2A_1 & R \leq -2 \end{cases}. \tag{11}$$

$$\Delta K_{th} = \Delta K_0 \frac{\left(\frac{a}{a+a0}\right)^{\frac{1}{2}}}{\left(\frac{1-f}{(1-A_0)(1-R)}\right)^{1+C_{th}R}}. \tag{12}$$

where C, n, p, q, f are empirical material constants. Coefficients A_0, A_1, A_2 and A_3 are parameters associated with the stress state (sample thickness). The thickness effect is also considered by the apparent fracture toughness K_{crit}. Intrinsic crack length a_0 is set as 0.0015 in (0.0381 mm).

In the procedure of evaluating $(da/dN)_R$, one of the most important work is to calculate K_{res}. Both the Finite Element Method (FEM) and Weight Function Method (WFM) can be used [18]. It is worth mentioning that the RS will redistribute during the cutting of the specimens or during the self-balance procedure in the FE analysis. Therefore, it is of great importance to make sure that the distribution of RS in the FE model agrees reasonably with that in the specimen. The input and output RS in the example are given in Fig. 5. It can be seen that there is a difference in the input and output RS in the CT specimen. The input one is the same as that in MT specimen since CT specimen is cut from the MT specimen. The output RS is the redistributed result after making a slot in FE model, which is consistent with that in the actual CT specimen [7]. If the measured RS in CT specimen was input into the FE model, then the output RS would be much smaller than that in the actual specimen, which will lead to underestimation of K_{res}. K_{res} is subsequently calculated using soft package ANSYS. Calculated K_{res} distributions are also shown in Fig. 5 and compared with the WFM solution from [22]. Calculated Δ_1 values are illustrated in Fig. 6.

It can be seen from Fig. 5(a) that estimated Δ_1 varies with the specimen configuration and externally applied load. Fig. 5(b) indicates that for the MT specimens the ratio $\Delta_1/(da/dN)_b$ shows similar characteristic shape as the K_{res} distribution except for the case of $R = 0.6$. The influence of applied stress on Δ_1 will be discussed in Section 4. Evaluated Δ_1 for the CT specimen is negative indicating that crack growth rate in CT specimen is reduced remarkably due to the presence of residual stress.

(a)   (b)
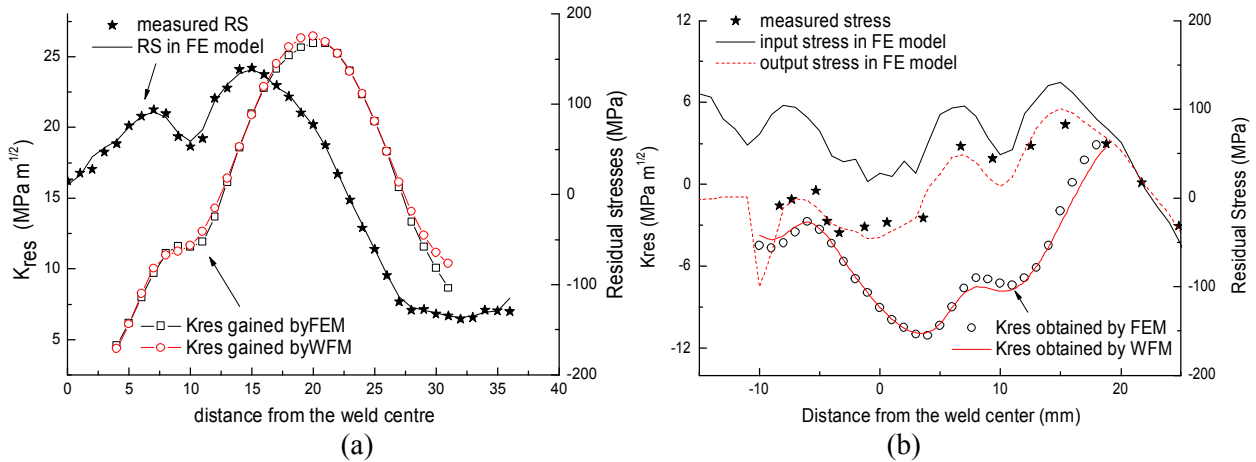
Figure 5.   Input, output RS and calculated K_{res} in (a) MT and (b) CT specimens

(a)   (b)
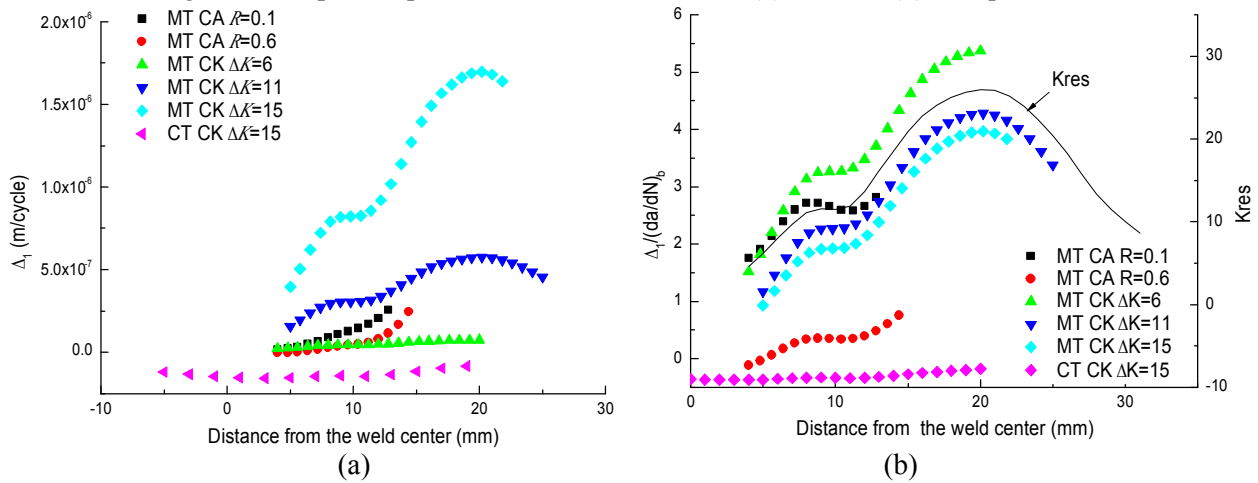
Figure 6. (a) Estimated Δ_1 and (b) ratio $\Delta_1/(da/dN)_b$

3.2. Evaluation of Δ_2

Since $(da/dN)_w$ is obtained by tests, $(da/dN)_R$ is calculated in section 3.1, Δ_2 can be evaluated by Eq. (9). The calculated results are given in Fig. 7. It can be seen from Fig. 7 that: (1) for the MT specimen with longitudinal weld (weld line parallel to the external stress), evaluated Δ_2 is lower than Δ_1 except the case ΔK=15MPa√m, which will be discussed in Section 4; (2) the ratio $\Delta_2/(da/dN)_b$ shows similar characteristic shape as the hardness variation.

(a)   (b)
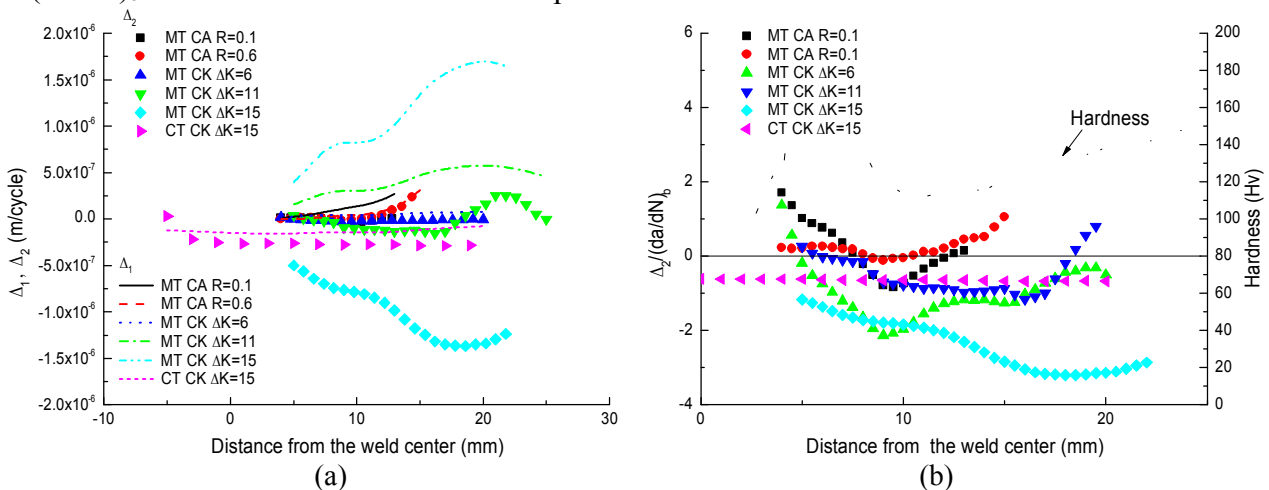
Figure 7. (a) Estimated Δ_2 and (b) ratio $\Delta_2/(\mathrm{d}a/\mathrm{d}N)_b$

4. Discussion on the Isolation Method

According to the results in Fig. 6 and 7, MT geometry is a better choice than the CT for isolating Δ_1 and Δ_2 in longitudinal weld specimen. Therefore, the following discussion is based on the MT configuration only.

4.1. Influence of applied stress level on isolation results

Evaluated Δ_1 and Δ_2 are functions of the externally applied stress, as shown in Fig. 6(a) and 7(a). Effect of applied stress on crack growth rate could be correlated by R_{app} and ΔK_{app}. Since $\Delta_1 = (\mathrm{d}a/\mathrm{d}N)_R - (\mathrm{d}a/\mathrm{d}N)_b$ and $\Delta_2 = (\mathrm{d}a/\mathrm{d}N)_w - (\mathrm{d}a/\mathrm{d}N)_R$, in which $(\mathrm{d}a/\mathrm{d}N)_w$ is test data, evaluated Δ_1 and Δ_2 depend on the calculation of $(\mathrm{d}a/\mathrm{d}N)_R$. Sensitivity analysis on the effects of R_{app} and ΔK_{app} on $(\mathrm{d}a/\mathrm{d}N)_R$ is carried out. For the discussion of the effect of R_{app}, constant ΔK loading condition is considered with the applied $\Delta K = 6$, 11, and 15 MPa√m, respectively. For the sensitivity of ΔK_{app}, three stress ratios are selected, i.e. $R = 0.1, 0.3, 0.6$. Sensitivity factors are obtained by taking the partial derivative of the output $(\mathrm{d}a/\mathrm{d}N)_R$ with respect to an input factor R_{app} or ΔK_{app}. The results are given in Fig. 8.

(a)   (b)
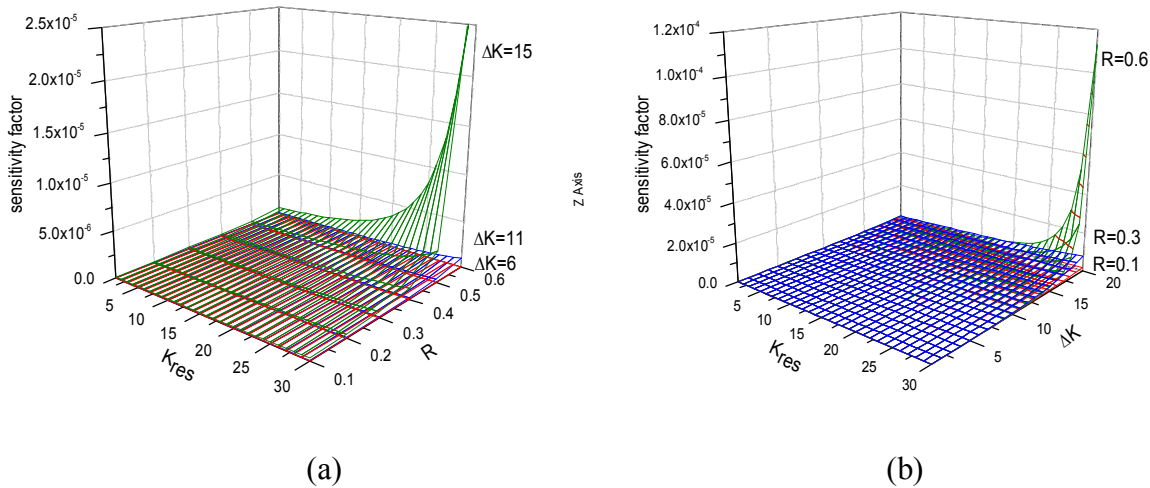
Figure 8.　Sensitivity analysis on (a) R_{app} and (b) ΔK_{app}

Fig. 8(a) indicates that if the applied ΔK level is low, e.g. 6 MPa√m, then calculated $(\mathrm{d}a/\mathrm{d}N)_R$ is not very sensitive to the stress ratio; if the applied ΔK level is high, e.g. 15 MPa√m, the sensitivity factor increases significantly with the increase of R_{app} and K_{res}. Fig. 8(b) tells that if R_{app} levels are keep low, e.g. below 0.3, $(\mathrm{d}a/\mathrm{d}N)_R$ is not very sensitive to ΔK_{app} level. Since $(\mathrm{d}a/\mathrm{d}N)_R$ represents the effect of RS on crack growth rate, it is expected that $(\mathrm{d}a/\mathrm{d}N)_R$ is sensitive to RS rather than applied stress. Therefore, high R ratios and high ΔK levels are not suitable for isolating Δ_1 and Δ_2.

4.2. Sensitivity analysis on K_{res}

Since K_{res} is calculated from measured RS distribution and scatter in RS data is unavoidable, it is unexpected that dispersion in RS data will introduce significant variation in the evaluated Δ_1 and Δ_2. Since K_{res} is calculated directly from RS, which keeps the error in RS, sensitivity analysis on the effects of K_{res} on $(\mathrm{d}a/\mathrm{d}N)_R$ is performed using the same method as in Section 4.1. Two kinds of externally applied stress are used, one is the CA condition of $\Delta\sigma = 35$ MPa and $R_{\mathrm{app}} = 0.1, 0.3$ or 0.5,

the result is given in Fig. 9(a); the other is the CK condition with ΔK levels of 6, 11, and 15 MPa$\sqrt{m}$, corresponding results are shown in Fig. 9(b).

<div align="center">(a)   (b)</div>
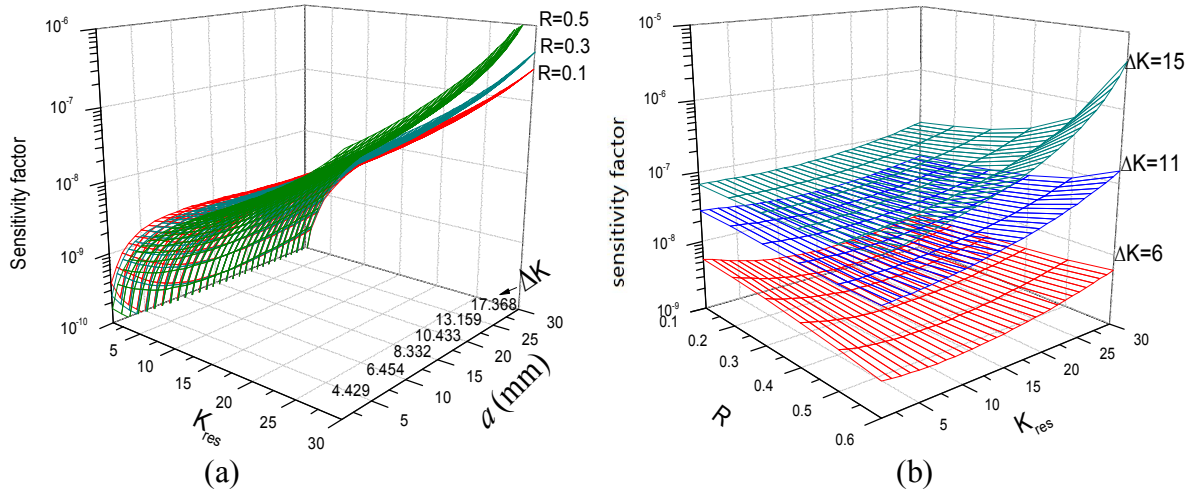
<div align="center">Figure 9.   Sensitivity analysis on K_{res}</div>

Fig. 9 indicates that the sensitivity factor of $(da/dN)_R$ with respect to K_{res} depends on the ΔK level significantly, while, R_{app} shows little effect on it. It is expected that $(da/dN)_R$ has certain sensitivity on K_{res} to reflect the effect of RS on crack growth rate, but sensitivity factor could better be kept in an acceptable level, otherwise, the error in measure RS data will show remarkable influence on the isolation results.

4.3. Influence of Crack Growth Laws on Isolation Results

The above discussions on the isolation method are all based on the NASGRO equation as shown in Eq. (10-12). Many other forms of crack growth rate correlation are available. Any crack growth law can be used in the isolation procedure if the parameters of R_{eff} and ΔK_{tot} are included in the equation. A popular and simple one is the Walker Equation [22] shown in Eq. (13).

$$\frac{da}{dN} = C(\Delta K (1-R)^{(m-1)})^n.$$

$\qquad(13)$

Let the crack growth rate in BM be described by the Walker equation in accordance with that in the NASGRO equation, parameters in the Walker equation are set as $C = 4.8 \times 10^{-11}$, $n=3.2$, $m=0.6937$, in unit of m and MPa. The loading case studied is the CA condition of $R = 0.1$, $\Delta\sigma_{app} = 35$ MPa. Comparison of $(da/dN)_b$ and $(da/dN)_R$ obtained by these two equations is shown in Fig. 10(a) and evaluated Δ_1 and Δ_2 are in Fig. 10(b). It is can be seen that: (1) $(da/dN)_R$ calculated by the two equations are slightly different, although $(da/dN)_b$ correlated by the two equations are almost the same; (2) $(da/dN)_R$ calculated by the Nasgro equation is a little higher than that by the Walker equation. This is because the effect of fracture toughness K_C is considered only in the Nasgro equation, and when $K_{max} + K_{res}$ is close to K_C, the Nasgro equation will give better prediction; (3) the evaluated Δ_1 and Δ_2 by these two equations are the same in trends and show slightly difference in value, this difference could be covered by the scatter in crack growth rate; (4) the Walker equation is simple in format and easy for assessing the influence of applied and residual stresses, which is a good choice when the applied and residual stresses are in a acceptable level.
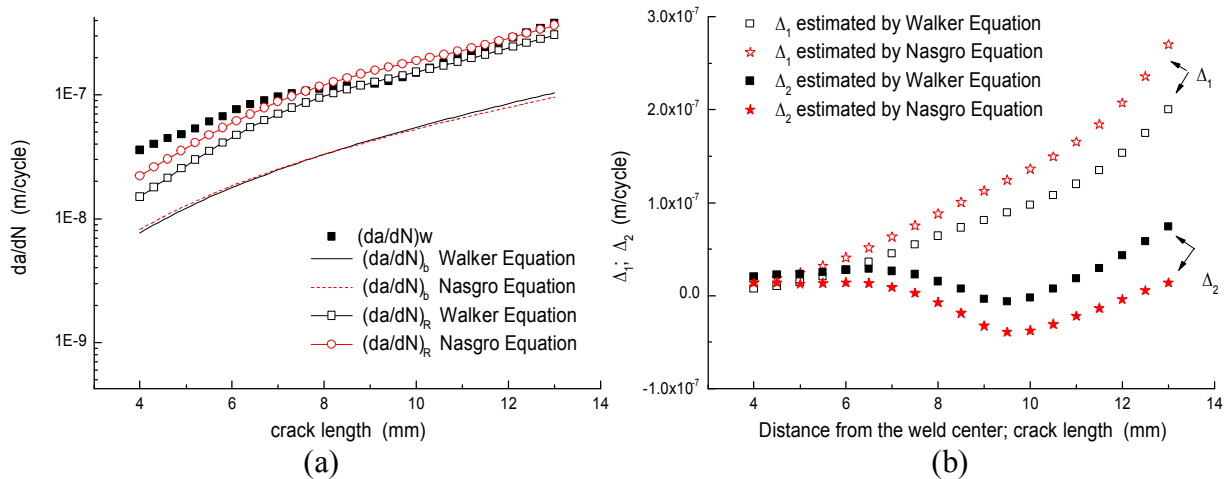
Figure 10. Comparison of the isolation results obtained by the Walker and Nasgro Equations

5. Conclusion

An isolation method for the contributions of residual stress and microstructural change in weld on fatigue crack growth rate is presented, and the factors affecting the isolation results are identified. It can be concluded that: (1) the presented method is applicable; (2) for specimens containing longitudinal weld, MT configuration is better than CT in the application of the isolation method; (3) the isolation results are found to be influenced by the test loading condition. High R_{app} or high ΔK_{app} are not good choice for studying the influential factors, but too low in R_{app} or ΔK_{app} can introduce crack closure in negative RS region, which is not good choice either; (4) if the applied stress is kept in a suitable level, a simpler crack growth law that include the effect of R and ΔK can be used in the presented method.

References
[1] C.Dalle Donne, G.Biallas, T.Ghidini, G.Raimbeaux. Effect of weld imperfection and residual stress on the fatigue crack propagation in friction stir welded joints.In:Proceedings of the second international symposium on friction stir welding, Gothenberg, Sweden,June 2000.
[2] R.John, K.V.Jata, K.Sadananda, Residual stress effects on near threshold fatigue crack growth in friction stir welds in aerospace alloys. Int J Fatigue, 25 (2003) 939-948.
[3] Y.C.Lam, K.S. Lian, The effect of residual stress and its redistribution on fatigue crackgrowth.Theor Appl Fract Mech, 12 (1989) 59-66.
[4] L.Fratini, S.Pasta, A.P.Reynolds, Fatigue crack growth in 2024-T351 friction stir welded joints: Longitudinal residual stress and microstructural effects. Int J Fatigue, 31 (2009) 495-500.
[5] R.Galatolo, A.Lanciotti, Fatigue crack propagation in residual stress fields of welded plates. Int J Fatigue, 19 (1997) 43-49.
[6] T.Ghidini, C.D.Donne, Fatigue crack propagation assessment based on residual stresses obtained through cut-compliance technique. Fatigue Fract Eng Master Struct, 30 (2007) 214-222.
[7] C.D.M.Liljedahl, J.Brouard,et al, Weld residual stress effects on fatigue crack growth behavior of aluminium alloy 2024-T351.Int J Fatigue, 31 (2009) 1081-1088.
[8] J.Christopher. Lammi, A.Diana. Lados, Effects of residual stress on fatigue crack growth behavior of structural materials:Analytical corrections. Int J Fatigue, 33 (2011) 858-867.

[9] G.Pouget, A.P.Reynolds, Residual stress and microstructure effects on fatigue crack growth in AA2050 friction stir welds. Int J Fatigue, 30 (2008) 463-472.

[10] G..Bussu, P.E.Irving, The role of residual stress and heat affected zone properties on fatigue crack propagation in friction stir welded 2024-T351 aluminium joints. Int J Fatigue 25 (2003) 77-88.

[11] K.V.Jata, K.K.Sankaran, J.J.Ruschau, Friction-stir welding effects on microstructure and fatigue of aluminium alloy 7050-T7451. Metallurgical and Material Transactions, 31A (2000) 2181-2192.

[12] Y.E.Ma, P.Staron., T.Fischer, P.E.Irving, Size effects on residual stress and fatigue crack growth in friction stir welded 2195-T8 aluminium-Part: Modelling. Int J Fatigue, 33 (2011) 1426-1434.

[13] C.D.M.Liljedahl, O.Zanellato, M.E.Fitzpatrick, J.Lin, L.Edwards, The effect of weld residual stresses and their re-distribution with crack growth during fatigue under constant amplitude loading. Int J Fatigue, 32 (2010) 735-743.

[14] G.Servetti, X.Zhang, Predicting fatigue crack growth rate in a welded butt joint: The role of effective R ratio in accounting for residual stress effect, 76 (2009) 1589-1602.

[15] M. A.Sutton, A.P.Reynolds, BC. Yang, R. Taylor, Mode Ⅰ fracture for 2024-T3 friction stir welds. Materials Science and Engineering A, 354 (2003) 6-16.

[16] J.A.Harter, AFGROW user guide and technical manual. AFRL-VA-WPTR-2008, XXXX,AFGROW for Windows XP /VISTA,Version 4.0012.15, July 2008.

[17] D.V.Nelson, Effects of residual stress on fatigue crack propagation. in: ASTM STP 776 American Society for Testing and Materials, Philadelphia, 1982, pp.172-194.

[18] R. Bao, X. Zhang, N. A. Yahaya, Evaluating stress intensity factor s due to weld residual stress by the weight function and finite element methods. Eng Frac Mechanics, 77 (2010) 3143-3156.

[19] R.Hou, D.M.Evans, J.C.McClure, A.C.Nunes, G.Garcia, Shielding gas and heat transfer efficiency in plasma arc welding. Weld J.75 (1996) 305-310.

[20] F.Lefebvre, Micromechanical assessment of fatigue in airframe fusion welds. PhD Thesis. University of Southampton, UK,2003.

[21] J.Brouard, J.Lin,P.E.Irving, Effects of residual stress and fatigue crack closure during fatigue crack growth in welded 2024 aluminium. In: Proceedings of fatigue, Atlanta, USA,June 2006.

[22] K.Walker, The effect of the stress ratio during crack propagation and fatigue for 2024-T3 and 7075-T6 aluminium.in: ASTM STP 462,Amrican Society for Testing and Materials, Philadelphia,1976,pp.1-14.